

Density Amplification in Laser-Assisted Protein Adsorption by Photobleaching

Jonathan M. Bélisle^{ab} and Santiago Costantino^{*abc}

^aMaisonneuve-Rosemont Hospital, University of Montreal, QC, Canada H1T2M4;

^bInstitute of Biomedical Engineering, University of Montreal, QC, Canada H3C3J7;

^cDepartment of Ophthalmology, University of Montreal, QC, Canada H3C3J7

ABSTRACT

Spatial distributions of proteins are crucial for development, growth and normal life of organisms. Position of cells in a morphogen gradient determines their differentiation in a specific manner. Neutrophils are the initial responders to bacterial infection or other inflammatory stimuli and have the ability to migrate rapidly up shallow gradients of attractants *in vivo*. Moreover, for the correct wiring of the nervous system, axonal growth cones detect concentration changes of specific proteins called guidance cues to navigate and reach their targets. Guidance cues can either be chemoattractive or chemorepulsive, and the same protein can act successively as both depending on the time point in development or the simultaneous presence of other molecules. A prerequisite to understand chemotaxis in a precise manner is the availability of a method able to reproduce *in vitro* the spatial distributions of proteins found *in vivo*. We recently introduced LAPAP (*Laser-assisted protein adsorption by photobleaching*), an optical method to produce substrate-bound protein patterns with micron resolution. Here, we present how the amount of protein present on the pattern can be increased by one order of magnitude.

Keywords: Protein patterning, photobleaching, density amplification

* Address correspondence to: santiago.costantino@umontreal.ca

1. INTRODUCTION

Distributions of protein are required for a myriad of processes occurring in living organisms. A particularly important process is axonal guidance which is needed to correctly wire the nervous system [1-3]. The growth cone is located at the tip the axon and extends and retracts filopodia to read information from molecular cues in order to guide the axon in the appropriate direction [4, 5]. Understanding axonal guidance is crucial for repairing central nervous system damaged nerves in order to guide axons back to their original target [6, 7]. Many other processes in development and normal life rely on distributions of proteins: morphogenesis [8, 9], angiogenesis[10], epidermal patterns[11], wound healing[12] and immune response [13].

Several methods have been developed to study cellular response to graded distribution of proteins *in vitro* [14, 15]. Traditional methods rely on diffusion to produce protein gradients such as the Boyden [16], Dunn [17] and Zigmond [18] chambers as well as biological hydrogels [19]. Micropipette generated gradients [20, 21] are produced in a more active manner since the volume of the puff, its frequency and the distance of the micropipette tip from the studied cells allows to modulate the produced gradient. New methods based on microfluidics have allowed producing user-defined protein patterns [22, 23]. Another one, based on microcontact printing, generated gradients from a macroscopic perspective by designing stamps with increasing spot size in one direction[24].

Recently, we introduced LAPAP [25], an optical protein patterning method which uses a low power laser to photobleach biotin-4-fluorescein (B4F) and adsorb it to a glass substrate. On-demand protein patterns can be obtained by scanning the laser beam while varying the laser intensity and the scanning velocity to modulate the amount of B4F adsorbed. Streptavidin is then incubated on the B4F pattern due to its strong affinity with biotin. The functionalization of the pattern can be done by then using biotinylated molecules or biotinylated antibodies and their antigens. The spatial resolution obtained with LAPAP is close to 1 μ m and the amount of bound protein can be modulated by three orders of magnitude. Using lasers of different wavelength and a mixture of antibodies conjugated with different dyes, it is also possible to produce two components protein patterns[26].

In order to speed up the photobleaching step, the method was improved by illuminating the whole field at once instead of scanning the laser beam, this method is called Widefield Illumination LAPAP[26]. Finally, using subsequent illumination of FITC conjugated antibodies against different targets; we were able to produce three component patterns.

To increase protein density that can be patterned, we present here an assay where the amount of streptavidin available to bind biotinylated antibodies is amplified [27].

2. MATERIALS AND METHODS

2.1 Experimental setup

The LAPAP setup (Fig. 1) used to produce protein patterns includes a 473 nm diode pumped solid state (DPSS) laser (Laserglow, ON, Canada) and intensities ranging from $0.1\mu\text{W}$ to $160\mu\text{W}$ are normally used. A 60x 1.2 NA water immersion objective (Olympus, Japan) is used to focus the laser beam at the interface of the coverglass and the solution of B4F. A xyz motorized translation stage (Thorlabs, NJ) is used to move the sample with respect to the focal spot of the laser. The laser power as well as the position of the sample is controlled by a home-made Labview (National Instrument, TX) program.

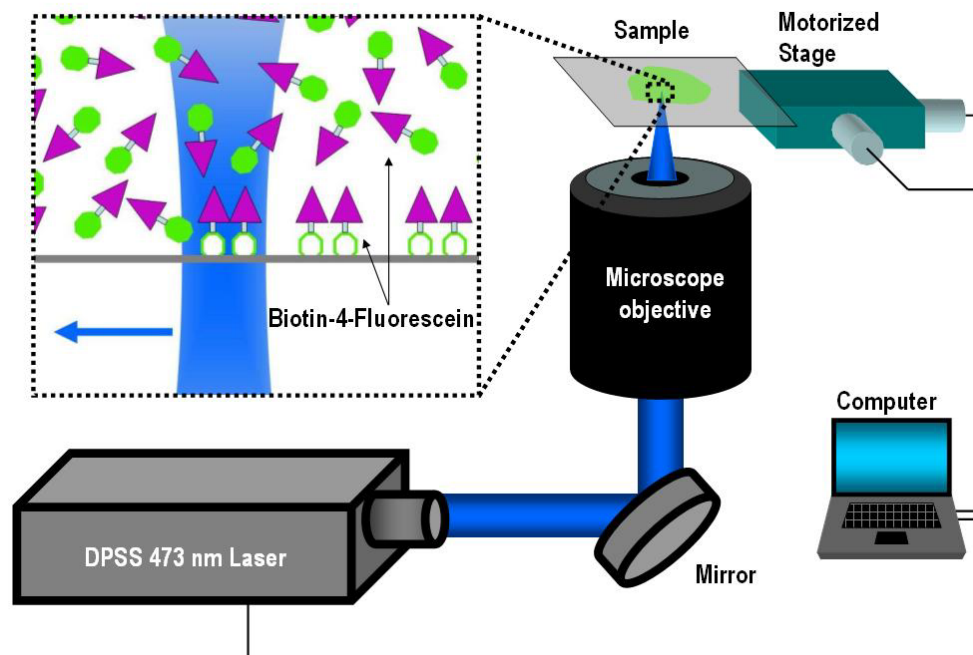


Figure 1. LAPAP setup includes a 473nm diode pumped solid state (DPSS) laser which is focused by a microscope objective on the top surface of a coverglass where a drop of biotin-4-fluorescein (B4F) is placed. The photobleaching of fluorescein binds B4F to the glass surface and a pattern can be created by scanning the laser across the surface while changing its intensity or velocity.

2.2 Patterning procedure

Protein patterns were produced on the coverglass of a 14mm glass-bottom-dish (MatTek Corporation, MA) on which a 3% bovine serum albumin (BSA) solution was incubated for 20 minutes in order to reduce the non-specific adsorption during the patterning step. The dish was then rinsed several times with PBS and positioned on the LAPAP setup (Fig. 1). A drop of B4F at $50\mu\text{g/mL}$ in 3% BSA was placed on the glass bottom dish and the photobleaching step was performed. A total of 15 squares $10\mu\text{m}$ long were patterned with a combination of 3 laser scanning velocities (2, 8 and $32\mu\text{m/s}$) and 5 laser powers (1.3 to $153.5\mu\text{W}$) in order to characterize density amplification. The dish was then rinsed several times with PBS to completely remove the unbound B4F. For standard patterns, $5\mu\text{g/mL}$ of streptavidin-Cy5 in 3% BSA was then incubated on the patterns for 30minutes. For density-amplified patterns, three consecutive 30 minutes incubation

steps of streptavidin, biotinylated rabbit anti-streptavidin antibody and streptavidin-Cy5 all at $5\mu\text{g}/\text{mL}$ in BSA 3% were performed. Figure 2 shows a schematic representation of the molecular structures obtained for both standard and amplification procedures. Graded patterns of proteins were also obtained with standard and amplified LAPAP.

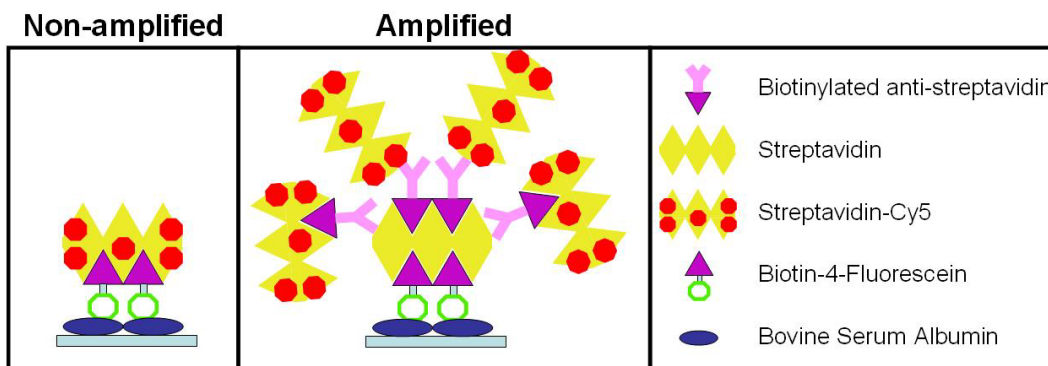


Figure 2. Schematic representation of standard and density amplified patterns obtained by LAPAP.

2.3 Image analysis

Images of standard and amplified patterns were acquired on an IX71 microscope (Olympus, Japan) equipped with a Retiga 2000R CCD camera (QImaging, Canada). To compare standard and amplified patterns, the gain and the exposure time of the CCD remained unchanged for all image acquisitions. The images were analyzed using ImageJ (<http://rsbweb.nih.gov/ij/index.html>) in order to measure the mean and standard deviation of the Cy5 fluorescence intensity in each of 15 patterned squares for both patterning procedures. No image modification or contrast adjustment were performed.

3. RESULTS AND DISCUSSION

3.1 Gradients

The gradients that were patterned (Fig. 3) show a clear amplification of the amount of Streptavidin-Cy5. For images acquired with the same parameters, the fluorescence from Cy5 is more intense from amplified patterns (Fig. 3b) compared to the intensity of non-amplified patterns (Fig. 3a).

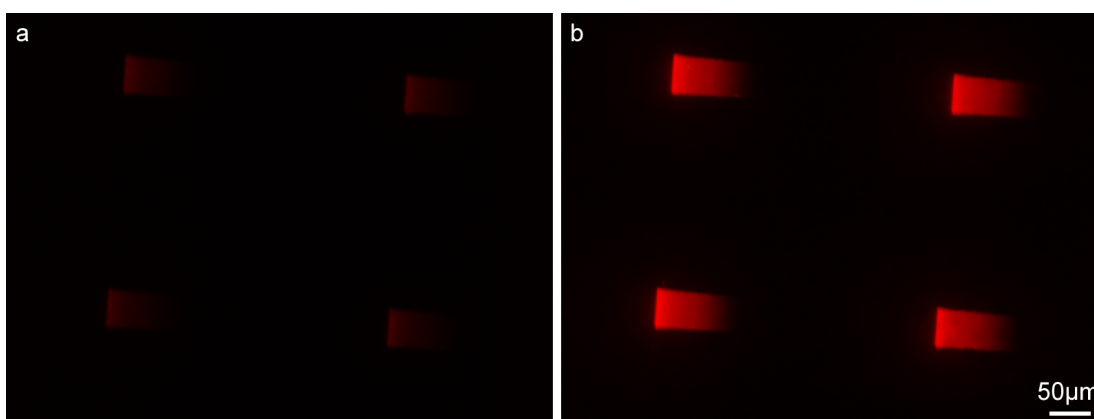


Figure 3. Streptavidin-Cy5 gradients obtained with (a) standard and (b) density amplification LAPAP. The camera gain and exposure time are the same for both images and no contrast adjustment was performed.

3.2 Characterization

We show Streptavidin-Cy5 fluorescence variation as a function of laser power for three different scanning velocities both for non-amplified and amplified patterns in Fig.4. Figure 4a shows that protein densities that before were only possible to achieve with very low scanning velocity ($2\mu\text{m/s}$) and maximum laser intensity ($153.5\mu\text{W}$) can now be easily achieved and surpassed at fast scanning velocity ($32\mu\text{m/s}$) by amplifying the patterns. It must be noted that a saturation of the amount of bound protein was previously observed for a laser powers of approximately $160\mu\text{W}$ in a detailed characterization of LAPAP [25].

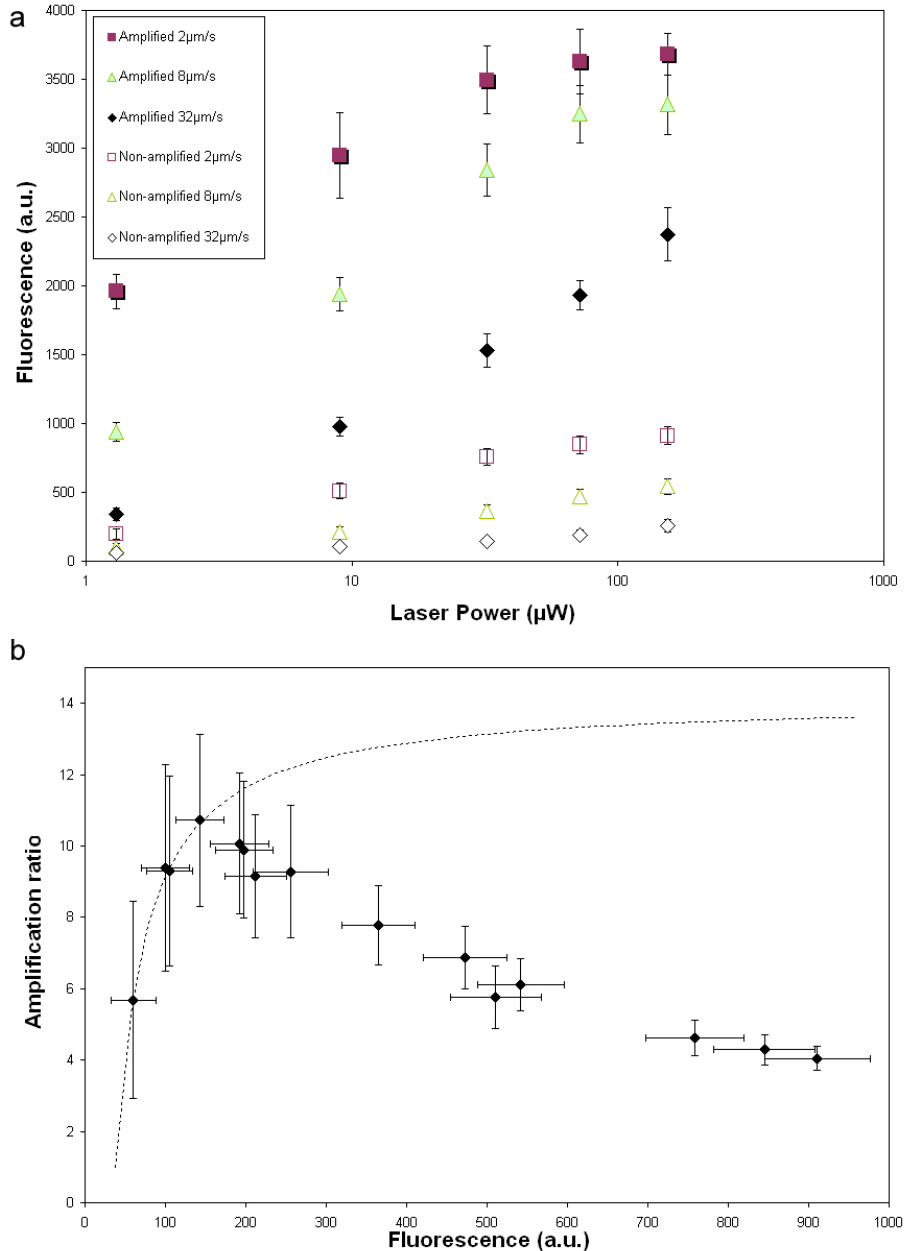


Figure 4. Amplification characterization. (a) Streptavidin-Cy5 density measured by the Cy5 fluorescence as a function of laser power at three different laser scanning velocities (2 , 8 and $32\mu\text{m/s}$) for both amplified and non-amplified patterns. (b) Amplification rate as a function of the non-amplified streptavidin-Cy5 amount measured by fluorescence.

Concentration gains were obtained based on fluorescence of streptavidin-Cy5. We plotted the fluorescence ratio amplified vs. non-amplified patterns (Fig. 4b). The result shows how our ability to increase the density decreases for high concentrations, since access to bound streptavidin becomes limited when the concentration is too high. On the other end, the amplification ratio seems also to decrease for low amounts of bound streptavidin (below a fluorescence value of 150). A simple model explaining this would be that the measured amplification ratio (K_{meas}) is a function of the fluorescence due to streptavidin-Cy5 (C_{Strep}), the fluorescence due to background noise (BG) and the real amplification ratio (K_{real}).

$$K_{meas} = \frac{K_{real} C_{strep} + BG}{C_{strep} + BG} \quad (1)$$

For low values of C_{Strep} , BG is a dominant term in Equation, for higher values of C_{Strep} , BG can be neglected and K_{meas} tends to K_{real} . In our experiment, BG was estimated by acquiring an image while no sample was on the microscope. We measured the mean fluorescence intensity of the image acquired and this yielded a BG value of 38. Based on this value, we evaluated K_{real} for the first four data point of Figure 4b and obtain an average value of 14.1 with a 0.3 standard deviation. The dashed line in Figure 4b represents ratio obtained from Equation 1 using these estimations of K_{real} and BG.

4. CONCLUSION

We have shown that amplification offers the possibility to reach higher protein concentration in patterns produced by LAPAP by only adding two incubation steps after the photobleaching procedure. Moreover, we showed that measured gains can reach a factor 10 depending of the initial protein amount.

5. ACKNOWLEDGEMENTS

This work is supported by the Natural Sciences and Engineering Research Council of Canada (NSERC), *Fonds québécois de la recherche sur la nature et les technologies* (FQRNT), Fonds de la recherche en santé du Québec (FRSQ) et la *Fondation de l'Hôpital Maisonneuve-Rosemont*.

REFERENCES

- [1] J. K. Chilton, "Molecular mechanisms of axon guidance," *Dev. Biol.*, 292(1), 13-24 (2006).
- [2] B. J. Dickson, "Molecular mechanisms of axon guidance," *Science*, 298(5600), 1959-64 (2002).
- [3] M. Tessier-Lavigne, and C. S. Goodman, "The molecular biology of axon guidance," *Science*, 274(5290), 1123-33 (1996).
- [4] D. Mortimer, T. Fothergill, Z. Pujic *et al.*, "Growth cone chemotaxis," *Trends Neurosci.*, 31(2), 90-8 (2008).
- [5] S. McFarlane, "Attraction vs. repulsion: the growth cone decides," *Biochem. Cell Biol.*, 78(5), 563-8 (2000).
- [6] P. J. Horner, and F. H. Gage, "Regenerating the damaged central nervous system," *Nature*, 407(6807), 963-70 (2000).
- [7] L. Olson, "Regeneration in the adult central nervous system: experimental repair strategies," *Nat. Med.*, 3(12), 1329-35 (1997).
- [8] H. L. Ashe, and J. Briscoe, "The interpretation of morphogen gradients," *Development*, 133(3), 385-94 (2006).
- [9] J. B. Gurdon, and P. Y. Bourillot, "Morphogen gradient interpretation," *Nature*, 413(6858), 797-803 (2001).
- [10] B. D. Wilson, M. Ii, K. W. Park *et al.*, "Netrins promote developmental and therapeutic angiogenesis," *Science*, 313(5787), 640-4 (2006).
- [11] S. Sick, S. Reinker, J. Timmer *et al.*, "WNT and DKK determine hair follicle spacing through a reaction-diffusion mechanism," *Science*, 314(5804), 1447-50 (2006).

- [12] G. C. Gurtner, S. Werner, Y. Barrandon *et al.*, "Wound repair and regeneration," *Nature*, 453(7193), 314-21 (2008).
- [13] C. R. Mackay, "Chemokines: immunology's high impact factors," *Nat. Immunol.*, 2(2), 95-101 (2001).
- [14] T. M. Keenan, and A. Folch, "Biomolecular gradients in cell culture systems," *Lab Chip*, 8(1), 34-57 (2008).
- [15] A. S. Blawas, and W. M. Reichert, "Protein patterning," *Biomaterials*, 19(7-9), 595-609 (1998).
- [16] S. Boyden, "The chemotactic effect of mixtures of antibody and antigen on polymorphonuclear leucocytes," *J. Exp. Med.*, 115, 453-66 (1962).
- [17] D. Zicha, G. Dunn, and G. Jones, "Analyzing chemotaxis using the Dunn direct-viewing chamber," *Methods Mol. Biol.*, 75, 449-57 (1997).
- [18] S. H. Zigmond, "Ability of polymorphonuclear leukocytes to orient in gradients of chemotactic factors," *J. Cell Biol.*, 75(2 Pt 1), 606-16 (1977).
- [19] H. Chen, Z. He, A. Bagri *et al.*, "Semaphorin-neuropilin interactions underlying sympathetic axon responses to class III semaphorins," *Neuron*, 21(6), 1283-90 (1998).
- [20] J. Q. Zheng, M. Felder, J. A. Connor *et al.*, "Turning of nerve growth cones induced by neurotransmitters," *Nature*, 368(6467), 140-4 (1994).
- [21] R. W. Gundersen, and J. N. Barrett, "Neuronal chemotaxis: chick dorsal-root axons turn toward high concentrations of nerve growth factor," *Science*, 206(4422), 1079-80 (1979).
- [22] N. L. Jeon, S. K. W. Dertinger, D. T. Chiu *et al.*, "Generation of Solution and Surface Gradients Using Microfluidic Systems," *Langmuir*, 16(22), 8311-8316 (2000).
- [23] D. Juncker, H. Schmid, and E. Delamarque, "Multipurpose microfluidic probe," *Nat. Mater.*, 4(8), 622-8 (2005).
- [24] A. C. von Philipsborn, S. Lang, J. Loeschinger *et al.*, "Growth cone navigation in substrate-bound ephrin gradients," *Development*, 133(13), 2487-95 (2006).
- [25] J. M. Belisle, J. P. Correia, P. W. Wiseman *et al.*, "Patterning protein concentration using laser-assisted adsorption by photobleaching, LAPAP," *Lab Chip*, 8(12), 2164-2167 (2008).
- [26] J. M. Belisle, D. Kunik, and S. Costantino, "Rapid multicomponent optical protein patterning," *Lab Chip*, 9(24), 3580 - 3585 (2009).
- [27] K. Hosokawa, and M. Maeda, "Spatial distribution of laminar flow-assisted dendritic amplification," *Lab Chip*, 9(3), 464-8 (2009).